Permeation and Sorption of CO_2 Through Amine-Contained Polyurethane and Poly(urea–urethane) Membranes

LIANG-SIONG TEO, JEN-FENG KUO,* and CHUH-YUNG CHEN

Department of Chemical Engineering, National Cheng Kung University, Tainan, Taiwan 70101, Republic of China

SYNOPSIS

As an absorbent of CO_2, tetraethylenepentamine (TEPA) and/or *N*-methyldiethanolamine (MDEA) was introduced into the hard segment as chain extenders of the series urethane polymer (PU), urea–urethane polymer (PUU), and segmented urethane/urea–urethane copolymer (SPU) based on 4,4′-diphenylmethane diisocyanate (MDI) and either poly(ethylene glycol (PEG)-400 or -600. The obtained polymers thus contained a nearly equal weight composition of both soft and hard segments and were prepared as polymer membranes for permeation and sorption of CO_2. The properties of the polymer membranes were characterized using a Fourier transform IR spectrophotometer, thermal gravimetric analysis, and rheometric measurement. The permeation and sorption isotherms as a function of temperature and pressure as well as the activation energy of permeability and diffusivity and the enthalpy change of the solution were measured. The test temperatures were carried out above and below the T_{gs} of soft-segment domains or the T_{gh} of hard-segment domains. The steady-state permeability (P) and diffusion coefficients (D) obtained ranged from 1.01 to 12.9 barrer and 1.04 to 4.04 cm^2/s, respectively, and the solubility coefficients (S), from 0.529 to 3.43 $cm^3(STP)/cm^3$ polymer-atm at 10 atm and 35°C. The TEPA-containing polymer membranes showed a smaller P and D but a larger S than did MDEA-containing ones. The membranes comprising PEG-600 exhibit the values of P, D, and S at about 11.5-, 2.5-, and 4.5-fold the PEG-400 ones, respectively. For SPU membranes, above T_{gs} or T_{gh}, the pressure dependencies of P followed the modified free-volume model. On the other hand, below T_{gs}, they exhibited a minimum permeability at a certain pressure caused by the plasticization action of sorbed CO_2. The sorption isotherms of CO_2 indicated that the membranes comprising PEG-400 can be described by a dual-mode sorption model below T_{gs}. Also, the SPU polymer membranes obied the Henry's law above T_{gs} as well as T_{gh}. The characteristic constants of the sorption model were also determined and are discussed.

INTRODUCTION

Carbon dioxide is a byproduct of numerous industrial processes. In view of the global warming and the recovery of CO_2 from other gas mixtures, the separation process with polymer membranes has attracted interest because it is less energy-intensive than are conventional processes such as the one used as a suitable solvent for the absorption of CO_2.[1]

The permeation of gases through polymer membranes depends strongly on whether the polymer is in its rubbery or glassy state. In general, the mechanisms of gas sorption in glassy polymers ($T < T_g$) is more complex than in rubbery polymers ($T > T_g$) because of their unequilibrium states[2,3]; i.e., the free segmental rotations of polymer chains are restricted below the T_g, resulting in the presence of microvoids or frozen "holes," and the sorption isotherms are concave to the pressure axis and have been successfully interpreted in terms of the dual-mode sorption model.[4–8] By contrast, because of the increase in the polymer segmental mobility above T_g,

* To whom correspondence should be addressed.

Journal of Applied Polymer Science, Vol. 59, 1627–1638 (1996)
 CCC 0021-8995/96/101627-12

the sorption isotherms become straight and can be described by the Henry's law. A number of investigators[9–12] have also reported that the Arrhenius plot of the permeability and diffusivity coefficients and the van't Hoff plot of the solubility coefficient for a given gas in a polymer exhibit a breakpoint near the T_g of the polymer.

Polyurethane is a segmented block copolymer composed of alternating aromatic urethane and macroglycol segments. Because of the incompatibility of the two dissimilar types of segments, it undergoes phase separation in which the urethane and the macroglycol segments cluster into hard and soft domains, respectively. Its properties are easily tailored by introducing controlled changes in the polyol chain length, chemical nature, and proportions of the constituents which make up the flexible and rigid segments of the polymer chain. This shows that the gas permeabilities of polyurethane membranes increases with the decrease of hard-segment content and the increase of soft-segment molecular weight.[13–16] In addition, the type of chain extenders[13,17] used also affect the permeation properties of the membranes with the result of changing the phase-separated morphology, crystallinity, density, and T_g of the membranes. Xiao et al.[14] observed that the Arrhenius relation of permeability deviates at above the temperature ranges of 60–80°C, which might be attributed to the increase of the mixing of hard and soft segments as a result of the dissociation of the short-range order in hard-segment domains. However, McBride et al.[18] showed a discontinuity in the Arrhenius plot of diffusivity at the onset of the glass transition in the hard domain. They suggested that the penetrants can diffuse through the hard domains at temperatures above the T_{gh} of the hard domains.

In this article, three series of urethane polymer (PU), urea–urethane polymer (PUU), and segmented urethane/urea–urethane copolymer (SPU) based on poly(ethylene glycol) (PEG)-400 or -600 and 4,4′-diphenylmethane diisocyanate (MDI) were prepared as polymer membranes for permeation and sorption of CO_2. As the chemical solvents of aqueous alkanoamines have been the most widely used as an absorbent of CO_2 in the acid gas treatment,[19] tetraethylenepentamine (TEPA) and/or *N*-methyldiethanolamine (MDEA) with a functional group of secondary and tertiary amines, respectively, were introduced into the hard segments as chain extenders of the polymers to interact with CO_2. The polymers were prepared to contain a nearly equal weight fraction of both hard and soft segments. The influence of the composition of both the hard and soft segments on the performances of permeation and sorption for CO_2 is focused on. The mechanism of CO_2 permeation and sorption isotherms of the polymer membranes were studied.

EXPERIMENTAL

Materials

The chemicals used for this study, as chain extenders, were 4,4′-diphenylmethane diisocyanate (MDI, Tokyo Kaisei Co., extrapure); poly(ethylene glycol) (PEG, Ferak Co.) of MW 400 and 600, used as polyols; *N*-methyldiethanolamine (MDEA, Merck Co., GC grade), and tetraethylenepentamine (TEPA, Ishizu Pharmaceutical Co., extrapure). The polyols were dried and degassed at 50°C under vacuum. *N,N*-Dimethylformamine (DMF, Katayama Chemical Co.) was dried by treatment with powdered magnesium sulfate and then stored over 4 Å molecular sieves before use. The other chemicals were used as received.

Synthesis of Polymers

The polymers used in this study were prepared by a two-step process. Polymerizations were conducted in a four-necked reaction kettle at 76°C under dry N_2. As usually used for the polymerization of urethane (U) or urea–urethane (UU), a prepolymer was prepared using MDI and PEG with a NCO/OH molar ratio of 2/1. DMF was used as the solvent. After the predetermined NCO content was reached, as determined by di-*n*-butylamine titratation,[20] the prepolymer was then chain-extented with a suitable amount of MDEA and/or TEPA to make the NCO/OH and/or NH_2 molar ratio 1/1 for yielding the final polymer. The polymer was precipated and then dried at 50°C under vacuum.

Preparation of Membranes

The polymers were dissolved in DMF to make 10% (by weight) solutions. The solutions were centrifuged at 2000 rpm to remove any gel particles or undissolved impurities for casting the membrane. The polymer membranes were made by putting a predetermined amount of the polymer solution on a clean polyethylene (PE) film supported with a glass cylinder which was covered with a filter paper to prevent any dust pollution. The system was placed in a nitrogen-purged oven at 80°C to cast the membrane. The polymer membrane was formed after

most of the DMF was removed. Then, it was removed from the PE substrate and put *in vacuo* at 50°C for about 3 days to remove the remaining solvent. The thickness of the dry membranes varied from 100 to 150 μm.

Characterization of the Polymer Membranes

The density of the polymer membranes was measured by the immersion method,[21] which included the weighing of the samples in air and in distilled water. Thermogravimetric analysis (TGA) was done on a DuPont-951 apparatus with a heating rate of 20°C/min under nitrogen purging. The IR spectra of thin membrane films were obtained with a Fourier transform IR spectrophotometer (Bio-Rad FTS 40A) at a resolution of 4 cm^{-1}. Dynamic mechanical measurements were made with rectangular specimens on a Rheometrics dynamic analyzer 700 (RDA-700) at 1 Hz in the temperature range −100 to 100°C at a heating rate of 5°C/min.

Permeation Measurement

The permeation of CO_2 through the polymer membranes was measured using the Barrer's high-vacuum technique.[22] The accumulative amount of gas passing through the polymer membrane in a constant volume receiving chamber (V) was measured by the pressure increase on the downstream side (p_d) with a pressure transducer (MKS Baratron 222B with a full-scale range of 10 Torr connected to an MKS Type PDR-C-1C readout). The upstream pressure (p_u) was monitored with a pressure transducer (Honeywell). The permeability coefficients (**P**) were then calculated by using the following equation:

$$\mathbf{P} = \frac{273 \times V \times L \times \frac{dp}{dt}}{760 \times T \times A \times (p_u - p_d)} \quad (1)$$

where $(dp)/(dt)$ is the gradient of the linear region (steady-state gas flow) of the p_d vs. time plot; L, the membrane thickness; T, the absolute temperature; and A, the membrane area, and p_d can be negligible ($p_d \ll p_u$).

The diffusion coefficients (**D**) were determined by the time-lag method[23] and represented as

$$\mathbf{D} = \frac{L^2}{6\theta} \quad (2)$$

where θ is the time lag which was the intercept obtained from extrapolating the linear region of p_d vs. the time plot to the time axis.

The solubility coefficients (**S**) can be calculated from the permeability equation of

$$\mathbf{S} = \frac{\mathbf{P}}{\mathbf{D}} \quad (3)$$

Sorption Measurement

The isothermal sorption of CO_2 in the polymer membranes was studied by a gravimetric method described elsewhere.[24,25] The sorption measurements in a polymer membrane were performed with a Sartorius electronic high-pressure ultramicrobalance Type S3D-P. The sensitivity of the microbalance was 0.1 μg. The weighing system was initially evacuated to 10^{-4} Torr until no change of the sample weight was registered. Subsequently, the vacuum source was shut off and the CO_2 was fed into the system, its pressure being measured with a pressure transducer (Honeywell). At any given pressure, the weight gain of the polymer membrane caused by absorption of CO_2 was allowed to attain a constant weight. Therefore, it allows one to determine the equilibrium sorption concentration of CO_2.

RESULTS AND DISCUSSION

Characteristics of the Polymer Membranes

The urethane polymer (PU), urea–urethane polymer (PUU), and segmented urethane/urea–urethane copolymer which is denoted as SPU were prepared as membranes for permeation and sorption of CO_2. The first one comprises either PEG-400 or -600 as the soft-segment and MDI–MDEA as the hard-segment ingredients; the second one comprises composites of MDI–TEPA as the hard-segment ingredients and the soft segment is the same as the first one; and the last one differed from the other two in that the chain extender used is composed of MDEA and TEPA with a mol ratio of 1/1. As shown in Table I, the weight ratios of the hard segment and the soft segment of those polymers studied are ca. 0.50–0.64, which are larger than those of usual polyurethanes. The use of MDEA and TEPA as the components of the hard domains is aimed to increase the affinity of polymer membranes to CO_2 by introducing those secondary and/or tertiary amine moieties. They are as follows:

Table I Characteristic of the Urethane and Urea–Urethane Polymer Membranes

Sample Designation	PEG (Wt %)	Density (g/cm^3)	Tan δ		TGA		X_B Fraction of Bonded Urethane Carbonyl
			T_{gs} (°C)	T_{gh} (°C)	T_d (°C)	Residue (%)	
PU-400	39.2	1.16	23.0	—	330	6.9	0.26
SPU-400	37.2	1.18	25.1	50.0	344	7.7	0.22
PUU-400	36.7	1.21	27.0	52.4	346	10.3	0.20
PU-600	49.2	1.04	−7.0	—	353	8.8	0.24
SPU-600	47.8	1.09	−3.9	25.2	355	9.5	0.23
PUU-600	46.5	1.12	−2.3	26.4	355	14.7	0.20

(1) PU-400 ; PU-600

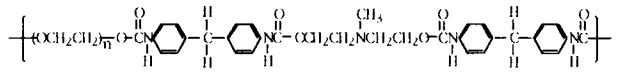

PEG soft segment MDI-MDEA-MDI hard segment

(2) PUU-400 ; PUU-600

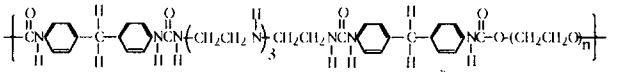

MDI-TEPA-MDI hard segment PEG soft segment

(3) SPU-400 ; SPU-600

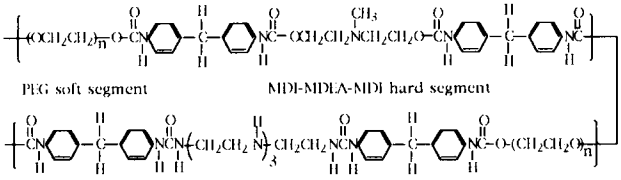

PEG soft segment MDI-MDEA-MDI hard segment

MDI-TEPA-MDI hard segment PEG soft segment

Among the polymers studied, the PEG-400-containing ones have a density around 1.18, slightly increasing with the TEPA content, while the PEG-600-containing ones have a density around 1.1, also increasing with increase of the TEPA content. This suggests that the PEG-600-containing membranes comprise more free volume than do the PEG-400-containing ones; meanwhile, the MDEA-containing PU comprise more free volume than do the TEPA-containing PUU and SPU. The decomposition temperature of the PU, PUU, and SPU membranes, T_d, was also determined using thermal gravimetric analysis. The PEG-600-containing polymer membranes have a T_d around 355°C, and the residue ranges from 8.8 to 14.7% by weight. Also, those PEG-400-containing ones have a T_d around 340°C, and the residue is 6.9–10.3%. The T_d and the residue increase with increasing of the TEPA content as well as of the PEG content. Thus, the introducing of TEPA improves the thermal stability of the polymer membranes. The membranes studied have a higher thermal stability property compared with the conventional polyurethane.[20]

Figure 1 shows the IR spectra of the PEG-400-containing polymer membranes. Very similar IR spectra are observed for the PEG-600-containing one. In both series, the membranes of PU-400 and PU-600 show the typical IR spectra of polyether-based PU[26]: a strong and sharp peak at 3313 cm^{-1} due to the stretching vibration of bounded NH; a strong absorption peaks at 1727 and 1710 cm^{-1} due to the stretching vibration of free and bounded C=O of urethane, respectively; and a C—O—C stretching vibration occurring at 1109 cm^{-1}, whereas for PUU as well as for SPU membranes, the IR spectra include a weak and broad peak at 3500 cm^{-1} due to the stretching vibration of free NH and a moderate strong peak at 1645 cm^{-1} due to the bounded C=O of urea[27,28] in addition to those of PU mentioned above.

Figure 1(a) illustrates that the IR spectra of the PUU-400 membrane measured the change of the intensities of both the peaks at 3500 and 3313 cm^{-1} as function of time under CO_2 atmosphere. The measurement was obtained by holding the polymer membrane in a sample chamber with NaCl windows (P/N 20.610, Graseby Specac Inc.) under CO_2 purging in the measurement period. The figure shows that the peak intensity of the free amine vibration at 3500 cm^{-1} decreases gradually with increasing time; meanwhile, the peak intensity of bounded amine at 3315 cm^{-1} increases, and then the former finally disappears. The phenomenon is attributed to the free amine groups of TEPA occurring at a specific interaction with CO_2 molecules.

The fraction of bounded C=O of urethane, X_B, relative to the free C=O of urethane is estimated by the following equation[28]:

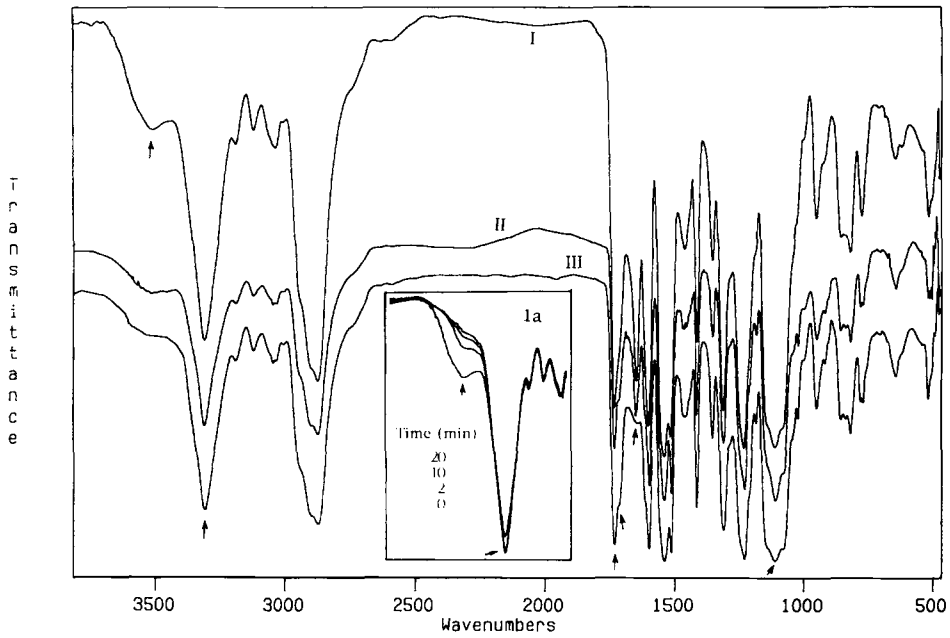

Figure 1 The IR spectra of the PEG-400-containing membranes: (I) PUU-400; (II) SPU-400; (III) PU-400. (1a) The change of the intensities of both peaks at 3500 and 3313 cm^{-1} as function of time under CO_2 atmosphere for PUU-400 membrane.

$$X_B = \frac{C_B}{C_F + C_B} = \frac{\dfrac{A_B}{\varepsilon_B}}{\dfrac{A_F}{\varepsilon_F} + \dfrac{A_B}{\varepsilon_B}} \tag{4}$$

and taking $\varepsilon_B/\varepsilon_F \cong 1.2$, where A, C, and ε are the absorbance, concentration, and extinction coefficient of bonded (B) and free (F) carbonyl groups, respectively, and are given in Table I. The fraction of bonded urethane carbonyls of the membranes studied is in a range from 0.20 to 0.26, increasing with increase of the TEPA moiety and decreasing with increase of the PEG length. As obtained above, the urethane or urea NH groups almost entirely involve hydrogen bonds. According to Tanaka et al.[29] and Seymour et al.,[26] the hydrogen bonds may form in polyether-based PU between the urethane NH groups as the proton donor and the urethane carbonyl and/or poly(ether oxygen) as the proton acceptor; the relative proportions depend on the composition and sample preparation. Therefore, for the PU membranes studied, the urethane NH groups (ca. 75%) essentially associate with the ether oxygen linkage, which makes the identity of hard-segment domains not quite obvious. The fact of the shift of the stretching vibration of C—O—C (Ref. 27) from 1113 to 1109.2–1108.8 cm^{-1} may be considered as other evidence. For PUU and SPU membranes, about 20–23% of urethane carbonyl groups are bonded to the urethane NH groups, similarly to the PU membranes; however, most urea carbonyl groups associate with hydrogen bonds with the urea NH groups in hard-segment domains, because one cannot find the peak at 1695 cm^{-1} due to the stretching vibration of free urea carbonyls instead of finding the peak at 1645 cm^{-1} due to the stretching vibration of bounded urea carbonyls. Thus, the steric hindrance of the bulky CH_3 groups in the hard segments that reduces the effectiveness of the hydrogen bonding within the NH and carbonyl of urethane groups may be taken less into account the fewer characteristics of hard-segment domains there are in the PU membranes.

Dynamic Mechanical Properties

As shown in Figures 2 and 3, the plots of the storage modulus (G') and the loss tan δ vs. temperature (T) of the polymer membranes are topically amorphous. The PU membranes exhibit a single dumping peak; on the other hand, the PUU and SPU show a dumping peak with a shoulder. For the latter two, the main dumping peak is attributed to the backbone motion of PEG-rich soft segments that accompany its glass transition, while the shoulder peak is related to the glass transition of the hard segments. The glass transition temperatures of the polymer membranes obtained are summarized in Table I. The

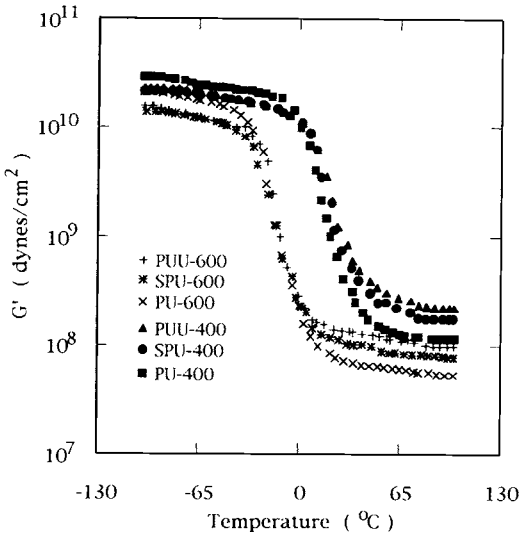

Figure 2 The plot of the storage modulus (G') vs. temperature for the urethane and urea–urethane polymer membranes.

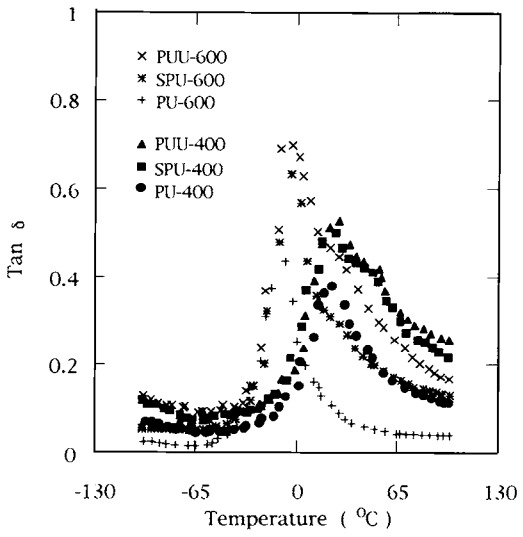

Figure 3 The plot of the loss tan δ vs. temperature for the urethane and urea–urethane polymer membranes.

larger the PEG, the lower the T_g. The PEG-600-containing PUU and SPU membranes show the T_{gs} of the PEG-rich soft-segment domains at around −3°C and the T_{gh} of the hard-segment domains at around 25°C. Also, those PEG-400-containing ones exhibit the T_{gs} at around 25°C and the T_{gh} at around 50°C. As compared with the T_g of PEG, which is ca. −40°C,[30] the relatively high T_{gs} obtained reveals a significant fraction of the component of the hard segment being dissolved in the PEG-rich soft-segment domains. The observations are consistent with those obtained by the IR studied. Note that in the glassy region the PU membranes have a larger G' than those of the other two membranes, and the latter two nearly have the same G'; in contrast, in the rubbery region, the G' of PU membranes is smaller than those of the other two membranes and the G' of PUU is larger. The former may be attributed to the relatively flexible hard-segment domains involved in the PUU and SPU membranes, because the hard segments of them are composed of a relatively long chain length of TEPA chemically linked with two units of MDI. The latter may take into account the character of the hard-segment domains of PUU or SPU still retained in the matrix at the rubbery state.

Permeation Properties

Figures 4 and 5 show the plots of the downstream pressure of CO_2 (p_d) vs. time (t) for the three series of polymer membranes at 35°C and the upstream pressure of 10 atm obtained by Barrer's high-vacuum technique.[22] Using eq. (1), one estimates the slope of the p_d vs. t plot at the steady state and then obtains the steady-state permeability coefficient (P). According to the time-lag method,[23] one determines the intercept of the slope of the p_d vs. t curve at the steady state with the abscissa and then substitutes in eq. (2) to obtain the diffusion coefficient (D). The test temperature is above the T_{gs} of these membranes but below the T_{gh} of the SPU-400 and PUU-400 membranes. Table II summarizes the values of P

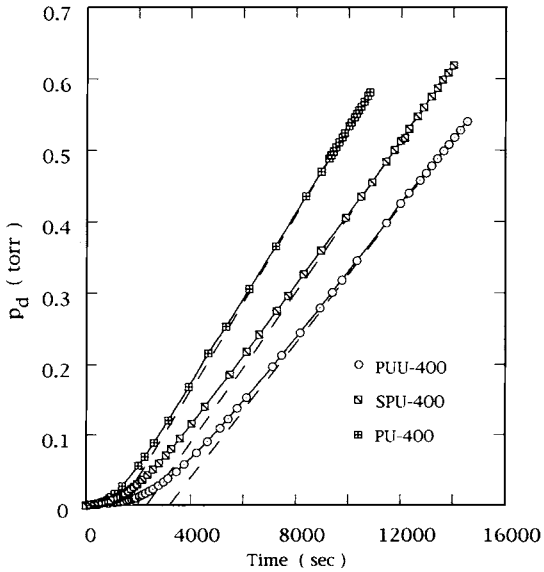

Figure 4 Time lag plot for permeation of CO_2 through PEG-400-containing membranes at 35°C and 10 atm.

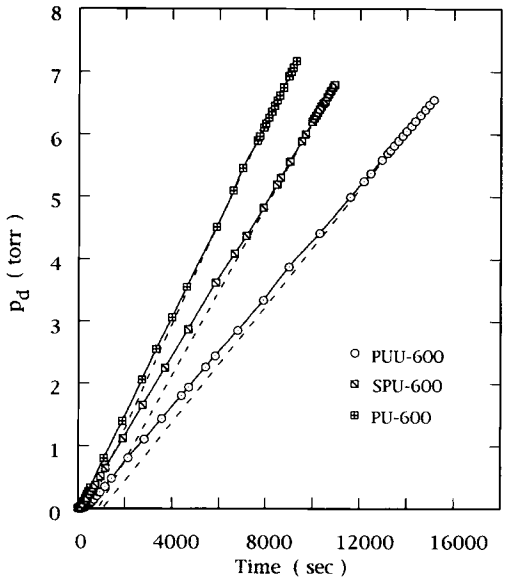

Figure 5 Time lag plot for permeation of CO_2 through PEG-600-containing membranes at 35°C and 10 atm.

and D as well as the solubility coefficient (S) obtained. The latter is obtained using eq. (3), i.e., $P = D \times S$. The performances of the membranes for permeation are comparable to those of the other polyurethane membranes.[15,16] Especially, the solubility of CO_2 is much more even. Obviously, the introduction of secondary and/or tertiary amine moieties improved the permeation properties of the polymer membranes. The PEG-400-containing membranes give a P value ranging from 1.01 to 1.12 barrer, a D value from 1.04 to 1.61 $\times$ 10^{-8} cm^2/s, and an S value from 0.529 to 0.738 $cm^3(STP)/cm^3$ polymer-atm, whereas for the PEG-600-containing ones, the P obtained is from 11.9 to 12.9 barrer, the D from 2.64 to 4.04 $\times$ 10^{-8} cm^2/s, and the S from 2.43 to 3.43 $cm^3(STP)/cm^3$ polymer-atm. Both P and D decrease with increase of the TEPA content; in contrast, the S increases with increase of the TEPA content. The latter may be owing to the interaction of free amine groups with CO_2, which has been shown by Figure 1(a), while the decrease of D with increasing TEPA content is probably due to the larger density of the TEPA membranes, i.e., the less free volume in the polymer matrix. Noteworthy is that the PEG-600-containing membranes show averaged P, D, and S values of about 11.5-, 2.5-, and 4.5-fold of the PEG400 ones, respectively. The increase of PEG content is the result of the improved permeation performance being more significant than the increase of NH groups in the hard segments. Thus, it indicates that most penetrant CO_2 mainly pass through the soft-segment domains.

Temperature Dependence

The temperature dependencies of P, D, and S vs. the reciprocal of absolute temperature ($1/T$) for CO_2 in the SPU polymer membranes at 1.2 atm are shown in Figure 6. The semilog plots of P and D vs. $1/T$ follow the Arrhenius relationship, while the semilog plots of S vs. $1/T$ obey the van't Hoff relationship. For SPU-400, every plot has a break at about 24°C, which is fairly close to the T_{gs} of the polymer membrane. It may be ascribed to the formation of Langmuir domains at the glassy state.[10] However, unlike the former, for SPU-600, those plots show a discontinuity at the temperature between 20° and 30°C. McBride et al.[18] also observed a discontinuity in the Arrhenius plots of ln D vs. $1/T$ for polyether-type PU in the glass transition region of the hard domain. Examining Figure 2, one finds that at the test temperatures of 10–20°C the

Table II Transport Coefficient and Dual-mode Sorption Parameters for CO_2 in the Urethane and Urea–Urethane Polymer Membranes

	Transport Coefficients[a]			Dual-mode Sorption Parameters[b]		
Sample Designation	P_{CO_2}	D_{CO_2}	S_{CO_2}	k_D	b	C'_H
PU-400	1.12	1.61	0.529	0.747	0.410	4.29
SPU-400	1.07	1.29	0.630 (0.637)[c]	0.990	0.831	3.17
PUU-400	1.01	1.04	0.738	1.21	1.14	2.39
PU-600	12.9	4.04	2.43	—	—	—
SPU-600	12.3	3.20	2.92 (2.95)	—	—	—
PUU-600	11.9	2.64	3.43	—	—	—

[a] Measured at 35°C and 10 atm. P: Barrer [10^{-10} $cm^3(STP)$ cm/cm^2 s cmHg]; D: 10^{-8} cm^2/s; S: $cm^3(STP)/cm^3$ polymer atm.
[b] Measured at 10°C. k_D: $cm^3(STP)/cm^3$ polymer atm; b: atm^{-1}; C'_H: $cm^3(STP)/cm^3$.
[c] Obtained from isotherm sorption experiments at 35°C.

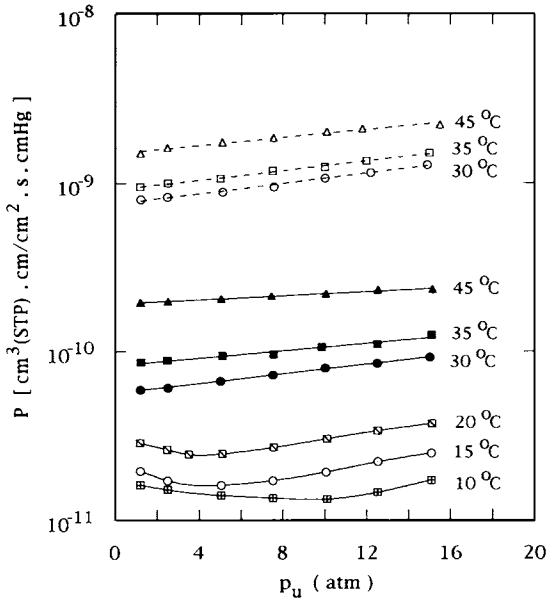

Figure 6 Upstream pressure dependence of permeability for CO_2 in SPU membranes at various temperatures: (solid lines) SPU-400; (dashed lines) SPU-600.

molecular chains of SPU-600 do not situate in the glassy state but, rather, in the real glassy transition between both the T_{gs} and T_{gh}, while those at 30–45°C completely fall in the rubbery plaateau region. This reveals that the mechanism of permeation of CO_2 through the polymer membrane at the glass transition state between the T_{gs} and T_{gh} is completely different from that through the membrane at the rubbery state. While the temperature is raised to near the T_{gh} of the hard domains, the hard domains begin to participate to some extent in the diffusion process. Because at $T > T_{gh}$ the intermolecular interaction force of hard-segment domains reduces significantly, and then the diffusion resistance of the hard-segment domains becomes less, the hard-segment domains therefore participate to a significant extent in the diffusion process.

From the slope of the lines in Figure 6, the enthalpy change of solution (ΔH_s) of the van't Hoff equation and the activation energy of diffusion (E_d) and permeation ($E_p = E_d + \Delta H_s$) of the Arrhenius equation as well as preexponential factors were obtained (Table III), respectively. The fact that $\Delta H_s < 0$ indicates that the heat of condensation is larger than the heat of mixing during the solution process of the CO_2; the results of $E_p > 0$ and $E_d > 0$ while $\Delta H_s < 0$ reveal that the activation energy barrier of diffusion is a dominant resistance for permeation of CO_2. Table III also indicates that the glassy state of the BPU-400 membrane shows a more exothermic solution and a smaller activation energy of diffusion

Table III Activation Energies of Permeation and Diffusion, Heat of Sorption[a] and Preexponential Factor[b] for CO_2 in SPU Polymer Membranes

		SPU-400	SPU-600
$T < T_{gs}$	E_p	6.69	—
	E_d	16.7	—
	H_s	−10.0	—
	P_0	2.78×10^{-6}	—
	D_0	6.56×10^{3}	—
	S_0	3.22×10^{-8}	—
$T_{gs} < T < T_{gh}$	E_p	15.5	5.75
	E_d	18.0	8.86
	H_s	−2.5 (−2.43)[c]	−3.11 (−3.26)
	P_0	9.15	2.15×10^{-5}
	D_0	6.59×10^{4}	1.06×10^{-1}
	S_0	1.06×10^{-2}	1.54×10^{-2}
$T > T_{gh}$	E_p	—	6.58
	E_d	—	12.0
	H_s	—	−5.42 (−5.49)
	P_0	—	5.00×10^{-5}
	D_0	—	8.62
	S_0	—	4.41×10^{-4}

[a] kcal/mol.
[b] P_0: cm³(STP) cm/cm² s cmHg; D_0: cm²/s; S_0: cm³(STP)/cm³ polymer atm.
[c] Obtained from isotherm sorption experiments.

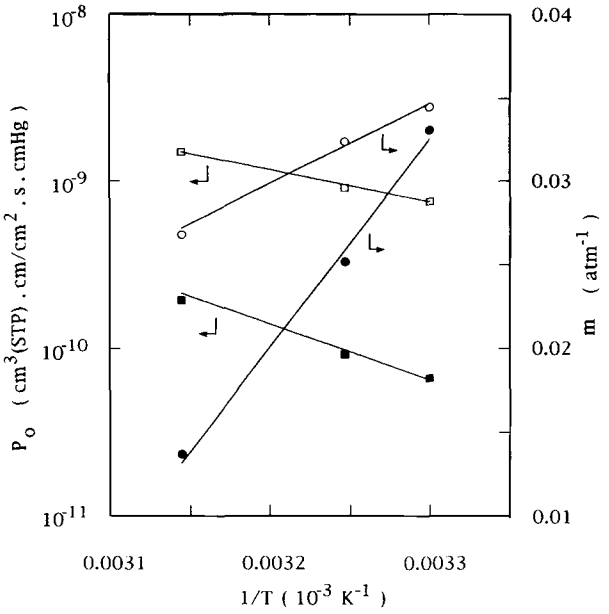

Figure 7 Temperature dependence of permeability at infinite dilution (P_0) and pressure sensitivity of permeability (**m**) for CO_2 in SPU polymer membranes: (closed symbols) SPU-400; (open symbols) SPU-600.

and permeation than those of the rubbery state and that the PEG-400-containing membrane exhibits a larger E_d and ΔH_s than that of the PEG-600-containing one.

Pressure Dependence

Figure 7 illustrates the semilog plot of P vs. upstream pressure (p_u) for SPU-400 and SPU-600 in the temperature range 10–45°C. As the test temperature is above the T_{gs}, SPU-400 shows a P value of about 0.8 to 2 barrer, increasing with p_u. However, when the test temperature is below the T_{gs}, P becomes about $\frac{1}{4}$–$\frac{1}{8}$-fold that above the T_{gs}, and the permeability first decreases with increasing p_u and then increases with increasing p_u. The p_u occurring as a minimum permeability is denoted as p_c and decreases with increase of the test temperature. The permeation behavior before p_c is similar to that of glassy polymer membranes; however, as $p_u > p_c$, it becomes like that of rubbery-state membranes. Therefore, a plasticization effect of CO_2 occurs as $p_u > p_c$, such that the plasticization of the polymer increases chain mobility substantially; thereby, the diffusivity of CO_2 increases with the sorbed concentration much more rapidly than the solubility decreases and then the permeability increases with the pressure. For SPU-600, all the temperatures studied are above the T_{gh}; the semilog plot of P vs. p_u is also found to increase linearly with increase of p_u. Accordingly,[31–33] such a linear relationship of the semilog plot of P vs. p_u above the T_g obtained indicates that the permeation of the membranes might be described by the modified free-volume model.

From Figure 7, one obtains, respectively, the intercepts (P_0) and the slopes (**m**) of the semilog plot of P vs. p_u for the runs above T_g. Physically, the P_0 and **m** are the permeability at infinite dilution and the pressure sensitivity of P, respectively. Figure 8 indicates that the temperature dependence of P_0 obeys the Arrhenius relation. The activation energy barriers of permeation at infinite dilution are 6.15 kcal/mol for SPU-600 and 15.8 kcal/mol for SPU-400, which are close to the E_p obtained at p_u = 1.2 atm (Table III). On the other hand, the **m** changes linearly and inversely with temperature. The tendencies for the temperature dependencies of P_0 and **m** are similar to that reported by Sada et al.[32,33]

Sorption Isotherm Below T_g

Figure 9 shows the sorption isotherms at 10°C as functions of CO_2 pressure for the PEG-400-containing membranes below the T_{gs}. Obviously, these isotherms exhibit a typical dual-mode sorption model,[4–8] i.e.:

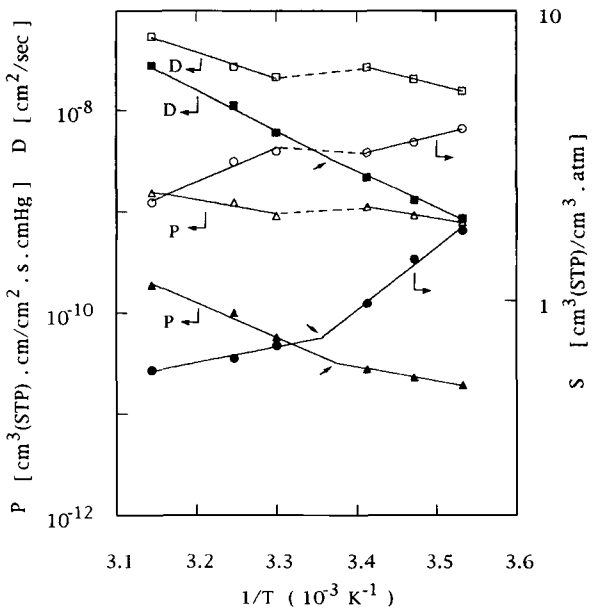

Figure 8 Temperature dependencies of permeability, diffusivity, and solubility of CO_2 in SPU polymer membranes: (closed symbols) SPU-400; (open symbols) SPU-600.

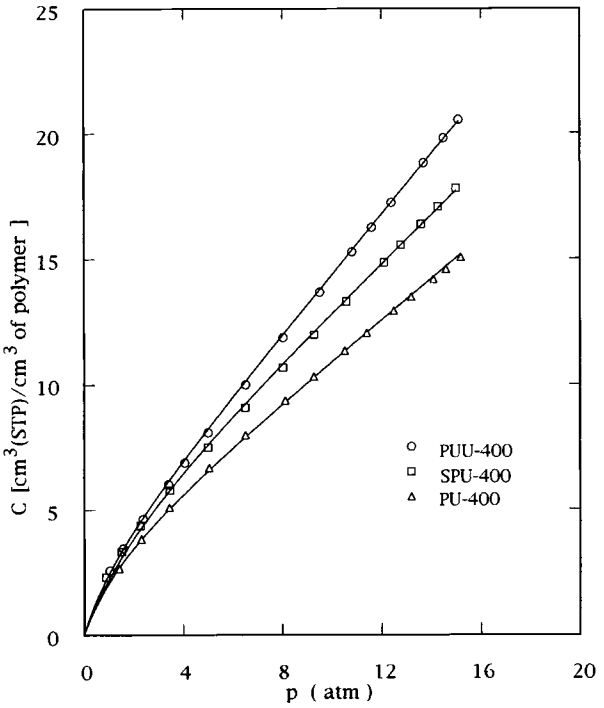

Figure 9 Sorption isotherms at 10°C as function of CO_2 pressure for PEG400-contained membranes.

$$C = C_D + C_H = k_D p + \frac{C'_H b p}{1 + bp} \tag{5}$$

As $bp \gg 1$, eq. (5) becomes

$$C = k_D p + C'_H \tag{6}$$

Also, the Langmuir sorption term (C_H) can be rearranged to be

$$\frac{p}{C_H} = \frac{1}{C'_H b} + \frac{p}{C'_H} \tag{7}$$

where the nomenclature used above is the same as reported elsewhere.[4] By using eqs. (6) and (7) along with the data of Figure 9, the characteristic constants of the dual-mode sorption model, k_D, b, and C'_H, are obtained (Table II). In this work, we recalculated the sorption isotherms, which are shown as the broken line, using the characteristic constants obtained from eq. (5). Obviously, the predicted sorption isotherms are in good agreement with the experimental values.

The Henry's constants k_D obtained are in the range 0.747–1.21 $cm^3(STP)/cm^3$ polymer-atm. Note that the secondary amine group-containing polymer membranes show a larger k_D than do the tertiary amine group-containing one. Also, the larger the TEPA content, the larger the k_D. It is attributed to a specific interaction of free secondary amines of TEPA with CO_2 as shown in Figure 1(a). The Langmuir mode affinity constant, b, is 1.14 atm^{-1} for PUU-400, 0.831 atm^{-1} for SPU-400, and 0.410 atm^{-1} for PU-400. The trend is the same as that of the Henry's constant just mentioned. Following the work of Muruganandam et al.,[8] one makes the plot of C'_H against ($T_g - T$), where T denotes the test temperatures for various high T_g polymers reported elsewhere[8,10,34,35] (Fig. 10). Obviously, the C'_H's of these glassy polymers approximately lie on the linear line of $C'_H = 0.159\ (T_g - T)$ with a standard deviation of 2.44. The C'_H's of PU-400, SPU-400, and PUU-400 obtained fall on the low bound of the line.

The temperature dependencies of the k_D and b of the SPU-400 membrane are found to obey the van't Hoff equation. The enthalpy change of the penetrant in the gas phase to the sorbed state in the Henry's law environment, ΔH_D, is obtained as −3.88 kcal/mol. Also, the enthalpy changes of the penetrant in the gas phase to the Langmuir sorbed state, ΔH_b, is obtained as −11.6 kcal/mol. The ΔH_b, being a third of the ΔH_D, indicates that the solution of CO_2 in the polymer matrix is less exothermic than is the adsorption of CO_2 on the surface of the microcavity. This is in agreement with the suggestion of Michaels

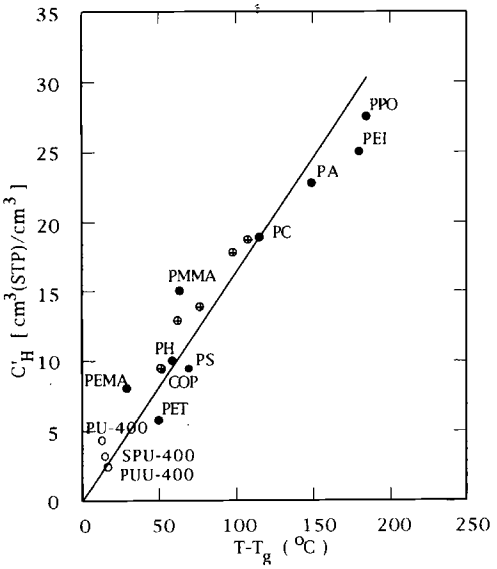

Figure 10 The plot of C'_H vs. ($T_g - T$) for various polymers. PET: poly(ethylene terephthalate)[10]; PEMA: poly(ethyl methacrylate); PMMA: poly(methyl methacrylate); PPO: poly(phenyl oxide)[8]; COP: copolyester[36]; PH: polyhydroxyether; PC: polycarbonate; PA: polyarylate; PEI: polyetherimide[35]; (⊕) PC/COP blends.[36]

et al.[36] They showed that for the Langmuir case, since microcavities supposedly already exist, no extra energy is required to separate chains enough to insert the sorbate molecule. The temperature dependence of C'_H is also satisfactorily described by the van't Hoff relation. The apparent enthalpy characterizing the temperature dependence of the Langmuir hole capacity[37] is obtained as −28.2 kcal/mol.

It is of interest to see that the T_{gs} of the membrane predicted by linear extrapolation to $C'_H = 0$ is 24.2°C, which is likely to correspond very roughly to the T_{gs} obtained by the dynamic mechanical analysis. It is consistent with the tendency of the C'_H to decrease with increasing temperature and to disappear near the glass transition temperature of the polymer.[38]

Sorption Isotherm Above T_g

Figure 11 shows the CO_2-sorption isotherms of the SPU polymer membranes as functions of pressure. The test temperatures are above the T_{gs}. All the sorptions obviously obey the Henry's law. In the temperature range studied, SPU-400 shows the k_D's in a range from 0.575 to 0.713 $cm^3(STP)/cm^3$ polymer-atm, decreasing with increase of temperature. However, the k_D of SPU-600 is about fivefold that of SPU-400. Therefore, the increase of PEG content is favorable for the solubility of CO_2. The k_D values at 35°C obtained here are the same as those obtained by the permeation study mentioned above. From the semilog plot of k_D against $1/T$, the enthalpy change of the CO_2 solution (ΔH_s) is −2.43 kcal/mol. Similar to the results of the permeation study, the van't Hoff plot shows a discontinuity at the temperature zone between 20 and 30°C. The ΔH_s are obtained as −3.26 kcal/mol in the temperature range of 10–20°C and −5.49 kcal/mol in the range 30–45°C. They are close to those obtained by the permeation study. Also, the sorption of CO_2 in the SPU-600 membrane is more exothermic than that of SPU-400.

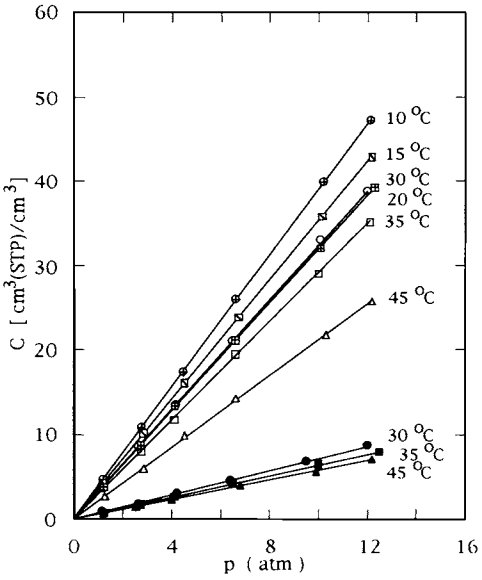

Figure 11 Sorption isotherms as function of CO_2 pressure for SPU polymer membranes above the glass transition temperature: (closed symbols) SPU-400; (open symbols) SPU-600.

CONCLUSION

In this work, the tertiary amine of MDEA and the secondary amine of TEPA and PEG-400 or PEG-600 were introduced into urethane and urea–urethane polymers as well as into segmented urea–urethane copolymers. The polymers thus obtained contain a nearly equal weight composition of hard and soft segments. The polymer membranes containing secondary amine exhibit a higher density, glass transition temperature, and thermal stability compared with those tertiary amine-containing ones. For the MDEA-containing polymer membranes, the bulky CH_3 groups of MDEA retards the formation of hydrogen bonds of the hard segments, leading to reducing the identity of hard-segment domains, whereas for the urea–urethane membranes, the secondary amine moieties retain the hard- and soft-segment domains as usual urethane polymers. The TEPA-containing membranes show a lower permeability and diffusivity but a higher solubility of CO_2 than do the MDEA-containing ones do. Noteworthy is that the improvement of the performances of permeation and sorption by increasing the PEG content is more obvious than that by the modification of the ingredients of the hard segment. Conclusively, the permeation of the penetrant CO_2 mainly passes through the PEG-rich soft domain. For SPU membranes, the permeation process above T_{gs} or T_{gh} shows the pressure dependencies of the permeability following the modified free-volume model. On the other hand, below T_{gs}, the plasticization effect of CO_2 strongly influences the permeation behavior that exhibits a minimum permeability at a certain upstream pressure. Although the SPU-600 membrane exhibits a rubberylike permeation and sorption above the T_{gs} or T_{gh}, the Arrhenius and van't Hoff plots show a discontinuity at temperatures between 20 and 30°C, but, rather, not a break in the SPU-400 membrane. This reveals that the permeation mechanism of CO_2 through the

SPU-600 membrane situated at the glassy transition between T_{gs} and T_{gh} is dissimilar to that at the rubbery state. The sorption isotherms of CO_2 for the PEG-400-containing membranes obey the dual-mode sorption model below T_{gs}. Also, the SPU polymer membranes obey the Henry's law above T_{gs} as well as T_{gh}.

The authors are grateful to the National Science Council of the Republic of China for its support in this work (NSC83-0405-E-006-146).

REFERENCES

1. G. Astarita, D. W. Savaga, and A. Bisio, *Gas Treating With Chemical Solvents,* Wiley, New York, 1983.
2. D. R. Paul and W. J. Koros, *J. Polym. Sci. Polym. Phys. Ed.,* **14,** 675 (1976).
3. R. T. Chern, W. J. Koros, E. S. Sanders, and R. Yui, *J. Membr. Sci.,* **15,** 157 (1983).
4. W. R. Vieth, J. M. Howell, and J. H. Hseih, *J. Membr. Sci.,* **1,** 177 (1976).
5. W. J. Koros, A. H. Chan, and D. R. Paul, *J. Membr. Sci.,* **2,** 165 (1977).
6. S. A. Stern and A. H. De Meringo, *J. Polym. Sci. Polym. Phys. Ed.,* **16,** 735 (1978).
7. P. Masi, D. R. Paul, and J. W. Barlow, *J. Polym. Sci. Polym. Phys. Ed.,* **20,** 15 (1982).
8. N. Muruganandam, W. J. Koros, and D. R. Paul, *J. Polym. Sci. Part B Polym. Phys.,* **25,** 1999 (1987).
9. W. H. Burgess, H. B. Hopfenberg, and V. T. Stannett, *J. Macromol. Sci.-Phys. B,* **5**(1), 23 (1971).
10. W. J. Koros and D. R. Paul, *J. Polm. Sci. Polym. Phys. Ed.,* **16,** 2171 (1978).
11. K. Toi, Y. Maeda, and T. Tokuda, *J. Membr. Sci.,* **13,** 15 (1983).
12. T. Hirose, K. Mizoguchi, and Y. Kamiya, *J. Appl. Polym. Sci.,* **35,** 517 (1988).
13. P. M. Knight and D. J. Lymam, *J. Membr. Sci.,* **17,** 245 (1984).
14. H. Xiao, Z. H. Ping, J. W. Xie, and T. Y. Yu, *J. Appl. Polym. Sci.,* **40,** 1131 (1990).
15. N. Cao, M. Pegoraro, F. Bianchi, L. Di Landro, and L. Zanderighi, *J. Appl. Polym. Sci.,* **48,** 1831 (1993).
16. G. Galland and T. M. Lam, *J. Appl. Polym. Sci.,* **50,** 1041 (1993).
17. K. H. Hsieh, C. C. Tsai, and D. M. Chang, *J. Membr. Sci.,* **56,** 279 (1991).
18. J. S. McBride, T. A. Massaro, and S. L. Cooper, *J. Appl. Polym. Sci.,* **23,** 201 (1979).
19. H. A. Al-Ghawas, D. P. Hagewiesche, G. Ruiz-Ibanez, and O. C. Sandall, *J. Chem. Eng. Data,* **34,** 385 (1989).
20. C. Hepburn, *Polyurethane Elastomers,* 2nd ed., Elsevier, London, New York, 1992.
21. ASTM Annual Book of Standards, D-792.
22. R. M. Barrer and G. Skirrow, *J. Polym. Sci.,* **3**(4), 549 (1948).
23. J. Crank, *The Mathematics of Diffusion,* Clarendon Press, Oxford, 1975.
24. A. R. Berens, *Angew. Makromol. Chem.,* **47,** 97 (1975).
25. S. Zhou and S. A. Stern, *J. Membr. Sci.,* **50,** 19 (1990).
26. R. W. Seymour, G. M. Estes, and S. L. Cooper, *Macromolecules,* **3,** 579 (1970).
27. H. Ishihara, I. Kimura, K. Saito, and H. Ono, *J. Macromol. Sci.-Phys. B,* **10**(4), 591 (1974).
28. C. B. Wang and S. L. Cooper, *Macromolecules,* **16,** 775 (1983).
29. T. Tanaka, T. Yokoyama, and Y. Yamaguchi, *J. Polym. Sci. Part A-1,* **6,** 2137 (1968).
30. J. A. Faucher and J. V. Koleske, *Polymer,* **9,** 44 (1968).
31. S. A. Stern and S. S. Kulkarni, *J. Polym. Sci. Polym. Phys. Ed.,* **21,** 467 (1983).
32. E. Sada, H. Kumazawa, Y. Yoshio, and S.-T. Wang, *J. Polym. Sci. Part B Polym. Phys.,* **26,** 1035 (1988).
33. E. Sada, H. Kumazawa, P. Xu, and S.-T. Wang, *J. Polym. Sci. Part B Polym. Phys.,* **28,** 113 (1990).
34. P. Masi, D. R. Paul, and J. W. Barlow, *J. Polym. Sci. Polym. Phys. Ed.,* **20,** 15 (1982).
35. T. A. Barbari, W. J. Koros, and D. R. Paul, *J. Polym. Sci. Part B Polym. Phys.,* **26,** 709 (1988).
36. A. S. Michaels, W. R. Vieth, and J. A. Barrie, *J. Appl. Phys.,* **34,** 1 (1963).
37. W. J. Koros, D. R. Paul, and G. S. Huvard, *Polymer,* **20,** 956 (1979).
38. W. J. Koros and D. R. Paul, *J. Polym. Sci. Polym. Phys., Ed.,* **19,** 1655 (1981).

Received June 26, 1995
Accepted August 30, 1995